Journal of Thermal Analysis and Calorimetry, Vol. 70 (2002) 841–852

PHASE TRANSITION OF LOCUST BEAN GUM–, TARA GUM– AND GUAR GUM–WATER SYSTEMS

S. Naoi [1], *T. Hatakeyama* [1*] *and H. Hatakeyama* [2]

[1]Otsuma Women's University, 1-2, Sanbancho, Chiyoda-ku, Tokyo 102-8357, Japan
[2]Fukui University of Technology, Gakuen, Fukui 910-8505, Japan

Abstract

Phase transition behaviour of neutral galactomannans, i.e., locust bean gum (LBG), tara gum (Tara-G) and guar gum (GG)–water systems is investigated. In this study, water content {W_c=(gram of water)/(gram of dry sample)} of these systems was varied from 0.2 to 3.6 g g^{-1}. In the DSC heating curves, glass transition (T_g), cold crystallization (T_{cc}) and melting (T_m) were observed in all three samples. In addition, liquid crystal transition (T^*) was observed in GG–water systems at a temperature higher than T_m. Using T_g, T_{cc}, T_m and T^*, phase diagrams of each system were established. From the melting enthalpy of ice in the systems, three types of water, non-freezing water (W_{nf}), freezing bound water (W_{fb}) and free water were calculated. The maximum amount of W_{nf} was observed at W_c=0.7 g g^{-1}, where T_g showed the lowest temperature. The amount of W_{nf} in LBG and GG is higher than that of Tara-G, whereas the highest amount of W_{fb} is found in GG. T^* was only observed in GG–water systems. It is concluded that frequency of the side chains in the repeating unit of the main chains of these three galactomannan affects the frozen structure of the glassy state in the presence of water.

Keywords: DSC, glass transition, guar gum, liquid crystal, locust bean gum, non-freezing water, phase transition, polysaccharide, tara gum

Introduction

Locust bean gum (LBG), tara gum (Tara-G) and guar gum (GG) are categorized as galactomannan polysaccharides which consist of a 1,4-β-*D*-mannose backbone and 1,6-α-*D*-galactose side chains. A structural difference among the three gums is the galactose/mannose ratio, which is 1:4, 1:3 and 1:2 for LBG, Tara-G and GG, respectively. These chemical structures are shown in Fig. 1. Gelation of the above three galactomannan polysaccharides in aqueous systems has been carried out by chemical modifications [1, 2], in the presence of cross linking agents [3–8], and mixing with other polysaccharides, such as xanthan gum and conjac mannan [9–12]. It has also been reported that LBG forms hydrogels by freezing and thawing process [13–15]. It is thought that regularly spaced side chains have a crucial role in gel forming ability [16].

* Author for correspondence: E-mail: hatakeyama@otsuma.ac.jp

1418–2874/2002/ $ 5.00
Akadémiai Kiadó, Budapest

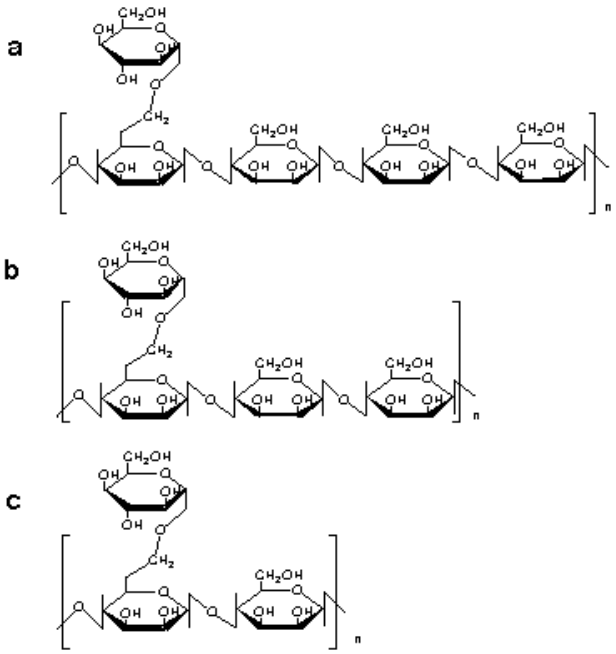

Fig. 1 Chemical structure of samples using this study; a – Locust bean gum, b – Tara gum, c – Guar gum

It is known that cross linking formation of polysaccharide physical hydrogels is mainly governed by chemical structure. At the same time, it is also reported that conformation of molecular chains of polysaccharides associated with water molecules is related with gel formation [17–20]. Hydrophylic groups, mainly hydroxyl groups in polysaccharide molecules are strongly bound with water molecules *via* hydrogen bonding. The molecular motion of the strongly bound water is different from that of pure water designated as non-freezing water [21]. The first-order phase transition is not observed for this kind of water. The number of non-freezing water molecules is closely related with number of hydrophylic groups of polysaccharides. By nuclear magnetic resonance spectroscopy (NMR), relaxation times of strongly bound water restrained by polysaccharide were reported [22, 23], i.e., ^{1}H longitudinal relaxation time (T_1) is $4.0 \cdot 10^{-1}$ s and ^{1}H transverse relaxation time (T_2) is $8.0 \cdot 10^{-2}$ s at 300 K. The NMR data indicate that the molecular mobility of non-freezing water is closer to that of solid polymers than that of water. The amount of non-freezing water is smaller than that of free water which is retained by cross linking networks. In addition to non-freezing and free water, there is a portion of water showing intermediate properties, i.e. the melting and crystallization temperatures of which are lower than those of pure water.

Recently, it was found that freezing bound water is related to biocompatibility and other functional properties, such as blood compatibility [24, 25]. Although phase transition of polysaccharides–water systems has been investigated by many researchers, the major part of reports are concerned with polysaccharide electrolyte–water

systems [22, 26–28]. In this study, the phase transition behaviour of a series of galactomannan polysaccharide–water systems was investigated using differential scanning calorimetry (DSC).

Experimental

Materials

Locust bean gum was obtained from Sigma Chemical Co., USA. The molecular mass was $3.1 \cdot 10^5$ according to the manufacturer. Tara gum and guar gum were provided by Fuso Kagaku Co. Ltd., Japan and Daiichi Kogyo Seiyaku Co. Ltd., Japan. The commercial names of Tara-G is Spino Gum and that of GG is DKS Fine Gum G-270. The samples were in powder form. LBG was white, Tara-G yellow white and GG light yellow.

DSC measurement

A Seiko Instruments Ltd. differential scanning calorimeter DSC 2000C equipped with a cooling apparatus was used. Scanning rate was 10°C min^{-1} and sample mass was about 3 to 5 mg. Nitrogen gas flow rate was 20 mL min^{-1}. Aluminium sealed type pans were used. Pans were weighed by a Sartorius microbalance with precision $0.1 \cdot 10^{-7}$. Samples were placed in the pans and a small amount of water was added using a micro syringe. The water was evaporated until an appropriate amount of water was attained. Then, the sample pans were sealed hermetically using an auto sealer. Sample with added water were weighed. Samples were kept at room temperature overnight in order to diffuse water into the powder samples. The above samples were again weighed in order to confirm that no mass loss occurred and the DSC measurements were carried out. The samples were heated to 60°C then, cooled at 10°C min^{-1} to –150°C. The samples were held at –150°C for 10 min, and heated to 60°C at the same rate. The above process was defined as the first run. The same measurement was carried out and defined as the second run. The results of the second run were used for analysis. The pans were pierced after DSC measurement, and then the pans were annealed at 120°C for 2 to 3 h in an electric oven. Water content (W_c) was defined as the following equation,

$$\text{Water content } (W_c) = (\text{g of water})/(\text{g of dry sample}), \ (\text{g g}^{-1}) \quad (1)$$

Glass transition temperature (T_g) was defined as the temperature at which the extrapolated baseline before the transition intersects the tangent drawn at the point of greatest slope on the step of the glass transition [29, 30]. Temperature and enthalpy of crystallization and melting of the sample were calibrated using indium and pure water as a reference. The heat capacity difference (ΔC_p) at T_g was calculated using the total mass of sample [31]. Peak temperatures were assigned as melting temperature (T_m), cold-crystallization temperature (T_{cc}) and liquid crystal transition temperature (T^*), respectively. The initial temperature of melting (T_{im}) was defined as the temperature where DSC curves deviates from the baseline. Temperature was calibrated using pure water and starting temperature of melting was determined as 0°C at heating rate of

10°C min^{-1}. Melting peak enthalpy (ΔH_m) was also calculated using pure water as a reference material. Freezing water (W_f) was evaluated using the following equation. W_f contains free water and freezing bound water (W_{fb}). Enthalpy of melting water (334 J g^{-1}) [32] was used for calculation.

$$\text{Freezing water } (W_f)=[(\Delta H_m)/334]/(m_{\text{dry sample}}) \quad (2)$$

where $m_{\text{dry sample}}$ is mass of dry sample. Non-freezing water was defined as follows,

$$\text{Non-freezing water } (W_{nf})=W_c-W_f \quad (3)$$

Morphological observations

Galactomannan–water systems were observed using a polarizing microscope (Leitz, Orthplan POL) at 25°C using a photo sensitive plate.

Result and discussion

Figure 2a shows DSC heating curves of LBG–water systems in a W_c ranging from 0.29 to 2.45 g g^{-1}. Glass transition temperature (T_g) is observed at ca –85°C for the samples with a W_c larger than 0.5 g g^{-1}, although T_g is not clearly seen in this figure. Magnified DSC curves are shown in Fig. 2b. An exothermic peak is observed at ca –20°C for the samples with W_c's 0.61 and 0.75 g g^{-1}. This peak is attributed to cold-crystallization temperature (T_{cc}). T_m is observed between –10 and 5°C for the samples with a W_c higher than 0.4 g g^{-1} and T_m shifts to the high temperature side with increasing W_c. T_{im}'s are observed at –35 to –10°C depending on W_c.

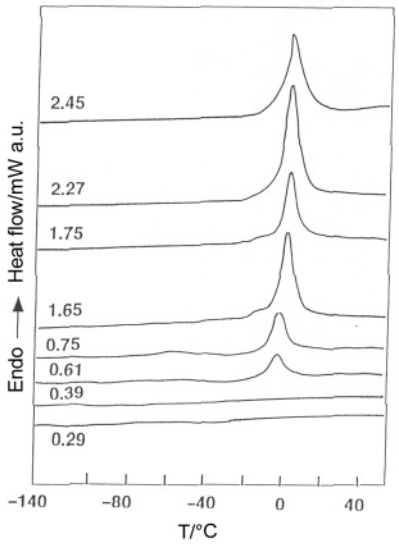

Fig. 2a Stacked DSC heating curves of LBG-water systems

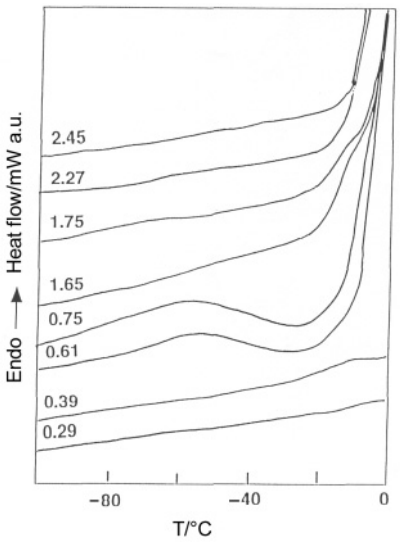

Fig. 2b Magnified DSC heating curves of LBG-water systems at –120–0°C

Figure 3 shows DSC heating curves of Tara-G–water systems in a W_c ranging from 0.62 to 3.63 g g^{-1}. T_g is observed at around –90°C for the samples with a W_c smaller than 1.4 g g^{-1} although T_g is not clearly seen in this figure. When DSC curves were magnified T_g and T_{cc} were clearly observed similar to those as shown in Fig. 2b. For the samples with a W_c ranging from 0.63 to 1.12 g g^{-1}, T_{cc} is found at ca –25°C. T_m is seen at ca 0°C for all samples and T_m shifted to the high temperature side with increasing W_c.

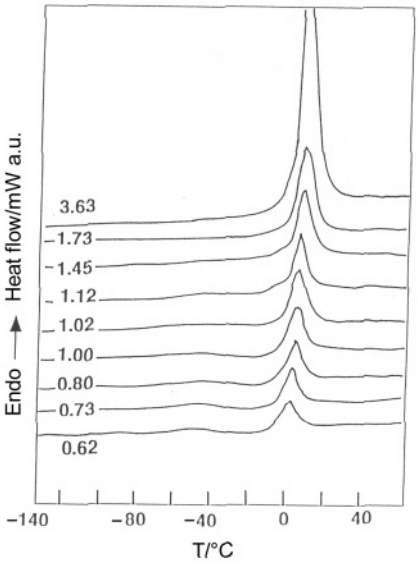

Fig. 3 Stacked DSC heating curves of Tara-G–water systems

Figure 4 shows DSC heating curves of GG–water systems in a W_c ranging from 0.22 to 2.68 g g^{-1}. T_g is observed at ca –80°C for the samples with a W_c larger than 0.22 g g^{-1}. T_{cc} is observed at ca –30°C for the samples with W_c higher than 0.22 g g^{-1} and T_{cc} shifted to the high temperature side. T_m is observed at ca 0°C, and T^* is observed at ca 20°C for the all samples except that having W_c=0.22 g g^{-1}. T_2^* is seen as a shoulder of T^* in the low temperature side when in a W_c ranging from 0.5 to 0.7 g g^{-1}. T_m shifts to the high temperature side with increasing W_c, on the other hand, T shifts to the low temperature side. T_m and T^* merge with each other.

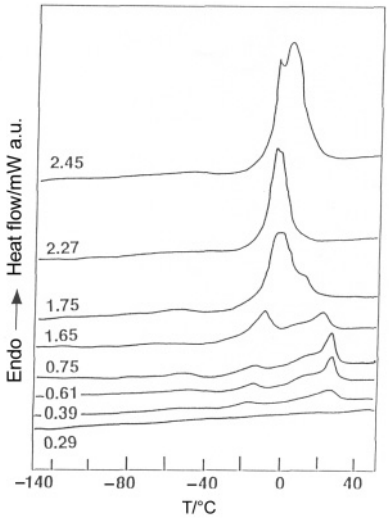

Fig. 4a Stacked DSC heating curves of GG–water systems

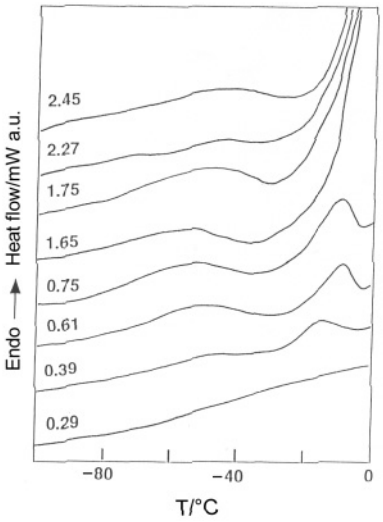

Fig. 4b Magnified DSC heating curves of GG–water systems at –120–0°C

The melting peak of LBG and Tara-G is observed as a single peak (Figs 2 and 3) and no endothermic peak was detected at a temperature higher than the melting peak. In contrast, in GG–water systems, an endothermic peak with a shoulder was observed at a temperature higher than melting. This peak is larger than the melting peak when W_c is lower than 0.63 g g^{-1} and peak temperature decreases with increasing W_c. The peak merges with the melting peak when W_c exceeds 1.4 g g^{-1}. By morphological observation, using a POL, a liquid crystal pattern was observed for the three samples at room temperature, however, in DSC measurements T^* was observed only for GG–water systems.

Phase diagrams established using phase transition temperatures of each system are shown in Figs 5, 6 and 7, respectively. T_g, T_{cc} and T_m are observed in all of the three samples. T_g and T_{cc} are found in W_c ranging from 0.5 to 1.0 g g^{-1} for LBG and Tara-G–water systems (Figs 5 and 6). On the other hand, in GG–water systems, T_g and T_{cc} are observed in a wide W_c ranging from 0.5 to 2.7 g g^{-1} (Fig. 7). As shown in Figs 5, 6 and 7, T_m is observed when W_c exceeds 0.4 g g^{-1} for all samples. T_m increased with increasing W_c, and leveled off at around W_c=1.0 to 1.2 g g^{-1}. Levelling off temperatures of the three samples are observed at 0°C. In the case of pure water, peak temperature of melting was observed at 5.4°C at the heating rate 10°C min^{-1} due to super-heating. The above facts suggest that freezing water coexists with a considerable amount of freezing bound water in these galactomannan–water systems.

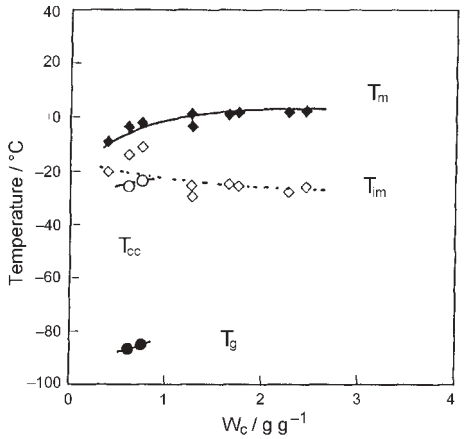

Fig. 5 Phase diagram of LBG–water systems; ● – T_g (glass transition temperature), o – T_{cc} (cold crystallization temperature), ◆ – T_m (melting temperature), ◇ – T_{im} (initial temperature of melting)

The fact that T_g and T_{cc} observed in a W_c ranging from 0.4 to 1.0 g g^{-1} where T_m is lower than 0°C suggests that water exists as freezing bound water in LBG– and Tara-G–water systems. In GG–water systems, T_g and T_{cc} were observed in a W_c ranging from 0.4 to 2.7 g g^{-1}. It is noted that the W_c range where T_g and T_{cc} are observed is affected by the frequency of side chains of the repeating unit of the sample. In GG–water system, the structural change of water that occurs is more pronounced than that of the other two systems.

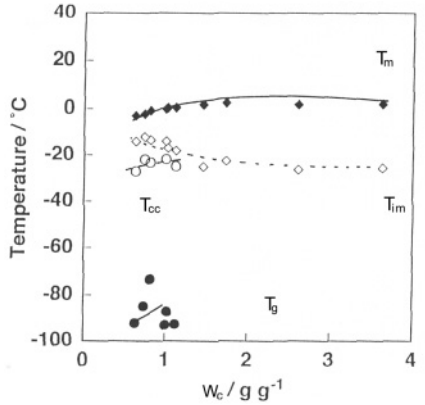

Fig. 6 Phase diagram of Tara-G–water systems; ● – T_g (glass transition temperature), o – T_{cc} (cold crystallization temperature), ◆ – T_m (melting temperature), ◇ – T_{im} (initial temperature of melting)

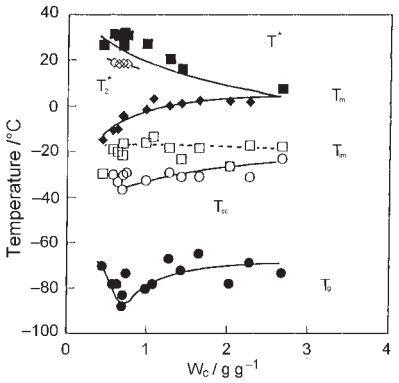

Fig. 7 Phase diagram of GG–water systems; ● – T_g, o – T_{cc}, ◆ – T_m, ■ – T_2^*, □ – T_{im}

Among three phase diagrams, T^* and T_2^* are only observed for GG–water systems. After referring to the established phase diagrams of other polysaccharides–water systems, such as cellulose sulfate [33], xanthan gum [34] and carboxymethylcellulose [35], T^* and T_2^* are assigned to liquid crystal transition. As shown in Fig. 4a and b, T^* is the peak of high temperature side, T_2^* is shoulder of T^*. This fact that two peaks are observed suggests the liquid crystalline state formed in GG–water systems is inhomogeneous. The inhomogeneous structure of the liquid crystalline phase has also been recognized in polystyrene sulfonate–water systems [26].

Figure 8 shows relationships between W_c and ΔC_p for all samples. Maximum point is seen at W_c=ca 0.7 g g^{-1}. This point corresponds to the minimum value of T_g in phase diagram of GG–water systems. As shown in Figs 5, 6 and 7, T_{cc} is necessarily appeared when T_g is observed. This indicates that molecular motion of galactomannan chains is enhanced cooperatively with bound water at T_g, and a portion of ice

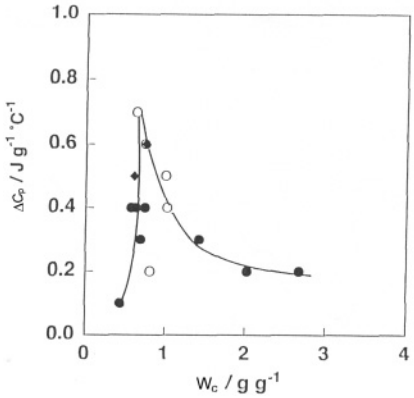

Fig. 8 Relationships between W_c and ΔC_p; ● – GG, o – Tara-G, ◆ – LBG

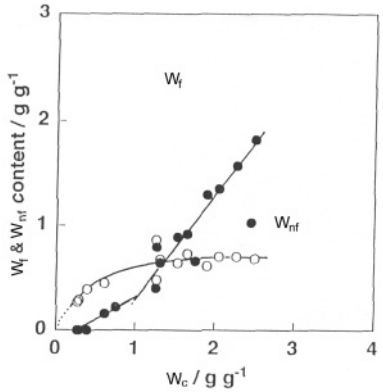

Fig. 9 Relationships between W_f, W_{nf} and W_c of LBG–water systems; ● – W_f (freezing water), o – W_{nf} (non-freezing water)

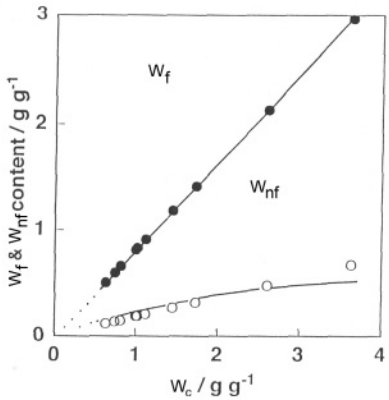

Fig. 10 Relationships between W_f, W_{nf} and W_c of Tara-G–water systems; ● – W_f (freezing water), o – W_{nf} (non-freezing water)

frozen in glassy state crystallizes at T_{cc}. When freezing ice is formed in the system, molecular mobility is restricted by the presence of ice. At the same time ΔC_p, an index of the amount of glass, decreases. ΔC_p decreases after passing the maximum point, and T_g increases with increasing W_c as shown in Fig. 7. In order to elucidate the molecular motion of frozen ice in the glassy state [36], further investigation is necessary in relation to super-cooling phenomena of water in the system.

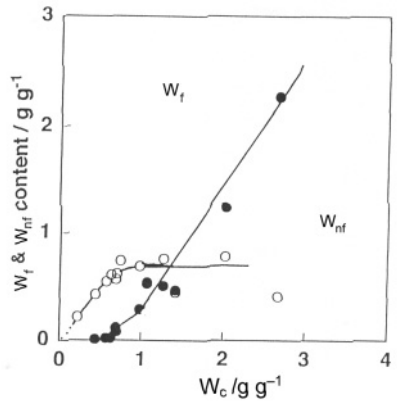

Fig. 11 Relationships between W_f, W_{nf} and W_c of GG–water systems; ● – W_f (freezing water), o – W_{nf} (non-freezing water)

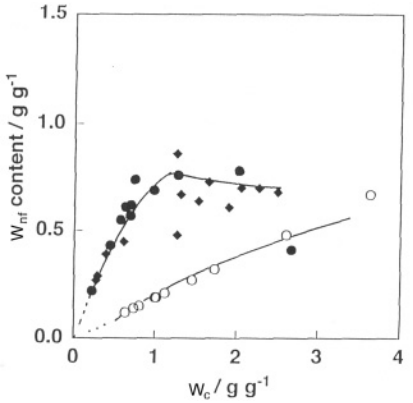

Fig. 12 Comparisons of W_{nf} among three samples; ● – GG, o – Tara-G, ◆ – LBG

Figures 9, 10 and 11 show the relationships between free water (W_f), non-freezing water (W_{nf}) and water content (W_c) for LBG, Tara-G and GG–water systems, respectively. W_{nf} increased with increasing W_c and levelled off at 0.7 g g^{-1}. The first-order transition was not detected when W_c was smaller than 0.4 g g^{-1} where water molecules are strongly bound by galactomannan chains and exist as non-freezing water. W_f shown in three figures contains a considerable amount of W_{fb} (freezing bound water) whose melting starts at –35 to –10°C as shown in DSC curves (Figs 2–4), and

phase diagrams (Figs 5–7). The gradient of W_f value in a W_c range from 0.4 to 1.0 g g^{-1} is smaller than that of high W_c range. This suggests that enthalpy of melting of W_{fb} is lower than that of free water.

W_{nf} of three samples is compared in Fig. 12. The highest amount of W_{nf} is found in LBG, while that of W_{fb} in GG. As reported previously [14], LBG forms hydrogels by freezing and thawing process, although no gels are formed for the other two samples. It is thought that hydrogel formation is affected by the amount of non-freezing water.

From the above facts, it is concluded that the phase transition behaviour of galactomannan–water systems is markedly affected by side chain structure. The amount of W_{nf} in LBG and GG is higher than that of Tara-G. In contrast, the amount of W_{fb} of GG was the highest. The liquid crystalline state was only observed in GG–water systems. It is noted that the frequency of the side chains of galactomannan affects the frozen structure in the glassy state in the presence of water.

* * *

The authors are grateful to Dr. S. Hirose, National Institute of Advanced Science and Technology for his helpful discussion. The authors wish to express their thanks to Fuso Kagaku Co. Ltd., Japan and to Daiichi Kogyo Seiyaku Co. Ltd., Japan for supplying the tara gum and guar gum samples, respectively.

References

1 S. Chakrabarti, D. Guillot and F. Rondelez, Polym. Prepr., 27 (1986) 247.
2 O. Noble, T. Turquois and F. R. Taravel, Carbohydr. Polym., 12 (1990) 203.
3 R. K. Prud'homme, V. Constien and S. Knoll, Polym., 223 (1989) 89.
4 O. Noble and F. R. Taravel, Carbohydr. Res., 184 (1988) 236.
5 C. Gey, O. Noble, S. Perez and F. R. Taravel, Carbohydr. Res., 173 (1988) 175.
6 S. Kesavan and R. K. Prud'homme, Macromolecules, 25 (1992) 2026.
7 E. Costell, M. H. Damasio, L. Izquierdo and L. Duran, Food Hydrocolloids, 6 (1992) 275.
8 E. Pezron, L. Leibler, A. Ricard and R. Audebert, Macromolecules, 21 (1988) 1126.
9 M. Tako and S. Nakamura, Carbohydr. Res., 138 (1985) 207.
10 P. B. Fernandes, M. P. Goncalves and J. L. Doublier, Carbohydr. Polym., 19 (1992) 261.
11 P. B. Fernandes, M. P. Goncalves and J. L. Doublier, Carbohydr. Polym., 22 (1993) 99.
12 K. P. Shatwell, I. W. Sutherland, S. B. Ross-Murphy and I. C. M. Dea, Carbohydr. Polym., 14 (1991) 115.
13 I. C. M. Dea, E. R. Morris, D. A. Ress and E. J. Welsh, Carbohydr. Res., 57 (1977) 249.
14 R. Tanaka, T. Hatakeyama and H. Hatakeyama, Polym. Int., 45 (1998) 118.
15 T. Hatakeyama, S. Naoi, M. Iijima and H. Hatakeyama, Biomacromolecules in submitting.
16 M. J. Gidley, G. Eggleston and E. R. Morris, Carbohydr. Res., 231 (1992) 185.
17 M. Takahashi, T. Hatakeyama and H. Hatakeyama, Carbohydr. Polym., 41 (2000) 91.
18 F. X. Quinn, T. Hatakeyama, H. Yoshida, M. Takahashi and H. Hatakeyama, Polym. Gels and Network, 1 (1993) 93.
19 F. X. Quinn, T. Hatakeyama, M. Takahashi and H. Hatakeyama, Polym., 32 (1994) 1248.
20 T. Yoshida, M. Takahashi, T. Hatakeyama and H. Hatakeyama, Polym., 39 (1998) 1119.
21 H. Hatakeyama and T. Hatakeyama, Thermochim. Acta, 308 (1998) 3.

22 T. Hatakeyama and H. Hatakeyama, in: W. G. Glasser and H. Hatakeyama (Eds) Viscoelasticity and Biomaterials, ACS Symp., 489 (1992) 329.
23 K. Hofmann and H. Hatakeyama, Polym., 35 (1994) 2749.
24 M. Tanaka, T. Motomura, N. Ishii, K. Shimura, M. Onishi, A. Mochizuki and T. Hatakeyama, Polym. Int., 49 (2000) 1709.
25 T. Hatakeyama and H. Hatakeyama, Hyluronan 2000, September, Wrexham, UK, Proceeding, 2000, p. 110.
26 T. Hatakeyama, H. Yoshida and H. Hatakeyama, Polym., 28 (1987) 1282.
27 T. Hatakeyama, H. Yoshida and H. Hatakeyama, Thermochim. Acta, 266 (1995) 343.
28 T. Hatakeyama, K. Nakamura and H. Hatakeyama, Kobunshi Ronbunshu, 53 (1996) 795.
29 T. Hatakeyama and F. X. Quinn, Thermal Analysis, John Wiley & Sons, Chichester 1998.
30 T. Hatakeyama and Z. Liu, Handbook of Thermal Analysis, John Wiley & Sons, Chichester (1998) p. 66.
31 H. Yoshida, T. Hatakeyama and H. Hatakeyama, in: W. G. Glasser and H. Hatakeyama (Eds) Viscoelasticicy and Biomaterials, ACS Symp., 489 (1992) 217.
32 J. A. Dean (Eds), Lange's Handbook of Chemistry 11th, McGraw Hill, 1973 p. 9.
33 T. Hatakeyama, H. Yoshida and H. Hatakeyama, Polym., 28 (1987) 1282.
34 H. Yoshida, T. Hatakeyama and H. Hatakeyama, Polym., 31 (1990) 693.
35 H. Hatakeyama and T. Hatakeyama, in: L. Salmen and M. Htun, (Eds) Properties of Ionic Polymer-Natural and Synthetic, STFI-Meddelande, Stockholm 1991, p. 123.
36 T. Hatakeyama, H. Yoshida, K. Nakamura and H. Hatakeyama, in N. Maeno and T. Hondho, (Eds) Physics and Chemistry of Ice, Hokkaido University Press, 1992, p. 262.